

# The influence of etch depth on electrical properties of solar cells

Rui Tong, Jiayi Liu & Stone Shih, Motech Renewable Energy Co. Ltd., Kunshan City, China

Fab & Facilities

Materials

Cell Processing

Thin Film

PV Modules

Power Generation

Market Watch

## ABSTRACT

In a multicrystalline silicon (mc-Si) cell production process, acid texturing is the most popular way of carrying out surface texturing. In general, the surface reflectivity and etch depth are the criteria used for quantifying the texture quality. In this study, four groups of cells were created with different etch depths of 2.82 $\mu\text{m}$ , 3.83 $\mu\text{m}$ , 4.41 $\mu\text{m}$  and 5.92 $\mu\text{m}$ . It was found that the etch depth had a notable effect on the efficiency of a cell. Also, the best texture was obtained with an etch depth of 4.41 $\mu\text{m}$ , at which there was a balance between a low reflectance and the removal of the saw-damage layer. As the etch depth increased, the film deposition thickness and the front bus-bar tensile strength were seen to increase. However, no linear relationship was found to exist between the diffusion sheet resistance and the etch depth.

## Introduction

In order to obtain high-efficiency solar cells, a light-trapping process is necessary [1]. The most common texturing technique is wet etching in a hot alkaline solution [2], which results in the formation of pyramids protruding from the silicon wafer surface. This surface structure has a very low reflectivity, but the wet-etching method is available only for <100>-orientation single-crystal Si wafers [2]. For multicrystalline silicon wafers (mc-Si) [1], alkaline texture solutions are unsatisfactory due to the existence of different crystal face grains. However, acid texture solutions have been successfully applied to mc-Si wafers and, because this method is low cost and suitable for mass production, it has been adopted for mass production of mc-Si wafers. In general, the mixture solutions (including nitride acid, hydrofluoric acid and deionized water) are used to etch an mc-Si wafer to obtain a surface that is covered in shallow pits, which improves the absorption of light and enhances the short-circuit current density of solar cells. Hauser [3] considers that a good texture needs a balance of low reflectance and the amount of damaged layer removed; the cause of dark lines on the mc-Si wafer surface and their influence on the efficiency of solar cells have been studied by Cao [4].

Texture conditions have a significant effect on the backend process and the efficiency of solar cells. In this paper, the variations of surface morphology with different etch depths are analyzed. The influences of morphology variations on diffusion, antireflective film deposition and bus-bar adhesion are also studied. Finally,

1	Pre-cleaning (4 groups)
2	Texture (measure etch depth and reflectance)
3	Diffusion (measure sheet resistance)
4	Edge isolation
5	PECVD (measure thickness of antireflective film)
6	Printing and firing (measure bus-bar tensile strength)
7	Cell test (measure electrical properties of cells)

Figure 1. Test process sequence.

the best etching depth is determined in relation to the efficiency of the solar cells.

## Experimental procedure

In this work, a selection of 156mm  $\times$  156mm boron-doped mc-Si wafers are used, having resistivities ranging from 0.8 to 3.0 $\Omega\text{cm}$  and thicknesses of (200 $\pm$ 10) $\mu\text{m}$ . The wafers are first immersed in an ultrasonic bath with a cleaning agent at 60 $^{\circ}\text{C}$  to remove any greasiness. In the second part of the procedure, the different etch-depth wafers are obtained by adjusting the process temperature and operating time of the texture machine. Making the solar cells in the next stage involves the following processes: diffusion, isolation, antireflective film coating,

electrode printing and co-firing. Finally, the cells' IV characteristic curves and electrical properties are determined using pulsed solar simulators and a measuring system.

The wafers are divided into four groups of different etch depths as shown in Table 1. The characteristic parameters of the different groups are analyzed in each process, according to the test sequence given in Fig. 1.

## Results and discussion

### Influence of etch depth on surface reflectance and texture profile

Measuring the saw-damage layer thickness is always a difficult task [5], but we were able to determine this value in our experiments. The etch depth is calculated from the etching quality and the area; for example, if the quality = 0.55g and the area = 156  $\times$  156 = 243.36 $\text{cm}^2$ , then the depth = [(0.55/2.33)/243.36]/2 = 4.85 $\mu\text{m}$  (where the density of Si = 2.33g/ $\text{cm}^3$ ). The surface profiles, observed by a scanning electron

Group	A	B	C	D
Etch depth [ $\mu\text{m}$ ]	2.82	3.83	4.41	5.92

Table 1. Etch depths of test groups.

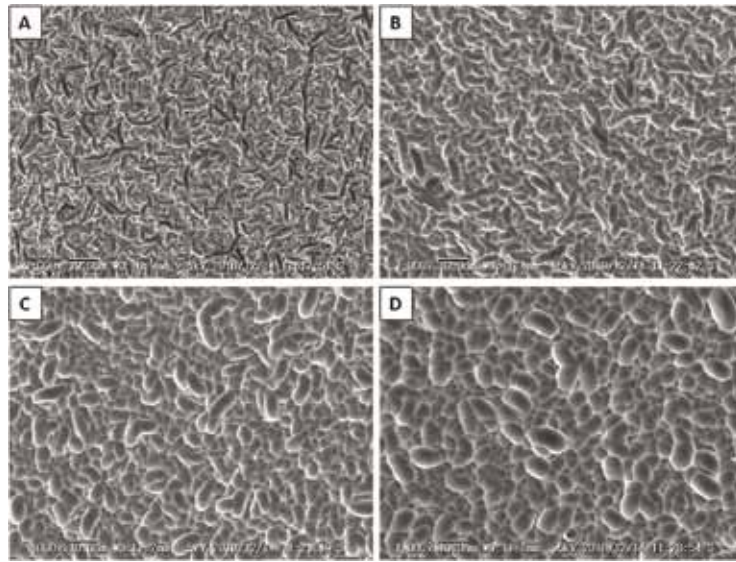


Figure 2. SEM images for samples of different etch depths: a) 2.82µm, b) 3.83µm, c) 4.41µm and d) 5.92µm.

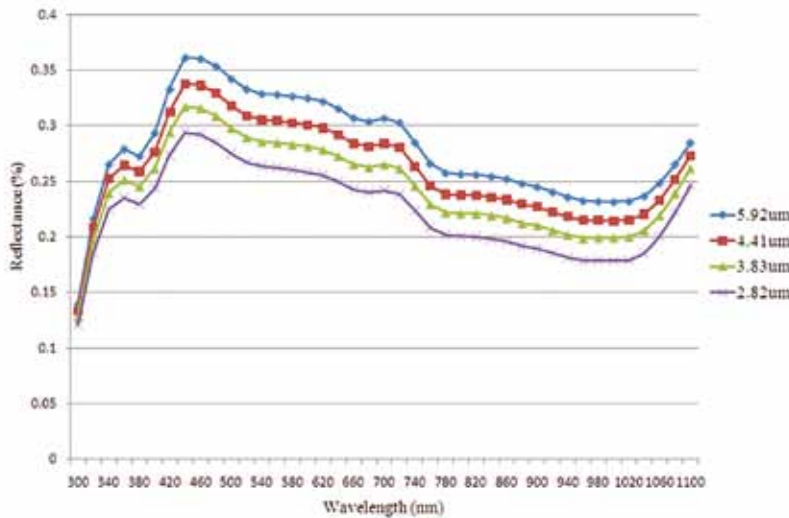


Figure 3. Surface reflectance at different wavelengths for etch depths of 2.82µm, 3.83µm, 4.41µm and 5.92µm.

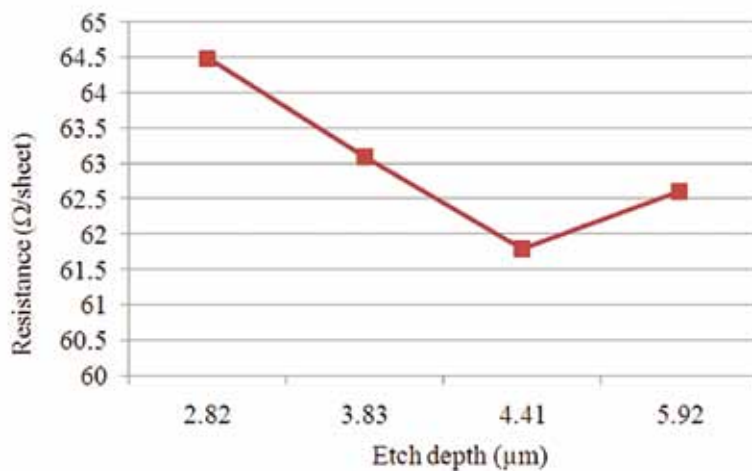


Figure 4. Sheet resistance for etch depths of 2.82µm, 3.83µm, 4.41µm and 5.92µm.

microscope (SEM), are shown in Fig. 2, and the surface reflectances, measured by the reflectance tool (ZOLIX Instruments SCS1011) at different wavelengths, are shown in Fig. 3.

Based on the SEM images, it is evident that the etch pits become larger as the etch depth increases. At the beginning of the reaction, the saw damage is the starting point of the reaction in the HF and HNO<sub>3</sub> mixture texture solution. The etch rate of the position of crystal dislocation is higher than the etch rate of other areas. So, as the etch progresses, the wafer surface forms long, narrow bow-like pits that have no specific orientation. These etch pits are similar in shape to crystal dislocation, but are much denser. As the etch depth increases further, the damage layer is completely removed, the etch rate becomes equal in all directions and the adjacent holes begin to merge. These factors finally cause the pits to become larger and circular, resulting in shiny wafers that can be observed by the naked eye. With increasing etch depth, the reflectance of the surface increases, causing greater loss of light.

#### Influence of etch depth on the diffusion sheet resistance

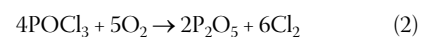
The test uses a tube diffusion machine to perform the phosphorus diffusion and a four-point probe (4pp) resistance measurement [6] to determine the sheet resistance ( $R_{sq}$ ). The results are shown in Fig. 4. It is seen that initially  $R_{sq}$  decreases as etch depth increases, but at an etch depth of 5.92µm,  $R_{sq}$  is increasing.

It was also found in our subsequent verification experiments that there is no clear relationship between  $R_{sq}$  and etch depth. According to Fick's first law:

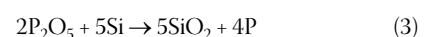
$$J = -D \frac{\partial c(x, t)}{\partial x} \quad (1)$$

the impurity diffusion current density  $J$  is proportional to the surface concentration gradient of the impurity. The diffusion coefficient  $D$  depends on the diffusion temperature, the type of diffusion impurities and the concentration of impurities, as well as other factors [7].

Liquid POCl<sub>3</sub> is used as the diffusion source and reacts with the oxygen in the tube at 800°C, according to the equation:



At the correct temperature, the reaction product P<sub>2</sub>O<sub>5</sub> reacts with the silicon and generates SiO<sub>2</sub> and phosphorus. This reaction equation is:



It can therefore be concluded that when POCl<sub>3</sub> and O<sub>2</sub> concentrations are saturated,  $R_{sq}$  depends on diffusion

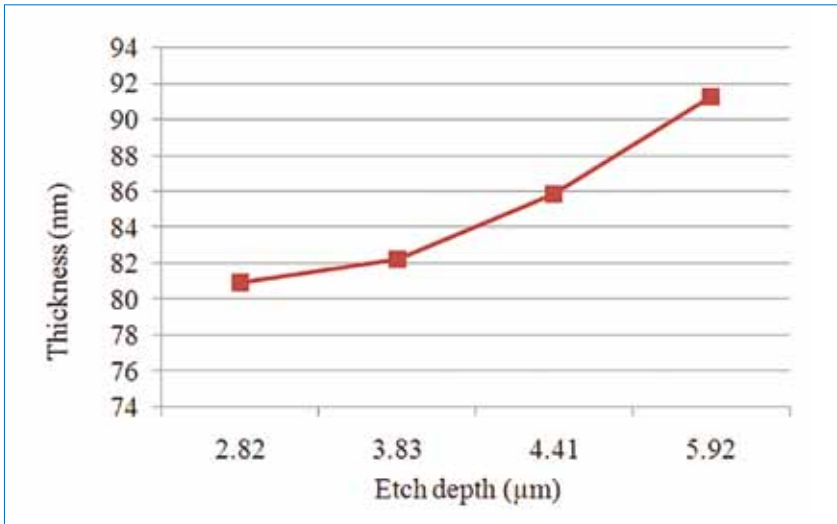


Figure 5. Antireflective film thicknesses for etch depths of 2.82μm, 3.83μm, 4.41μm and 5.92μm.

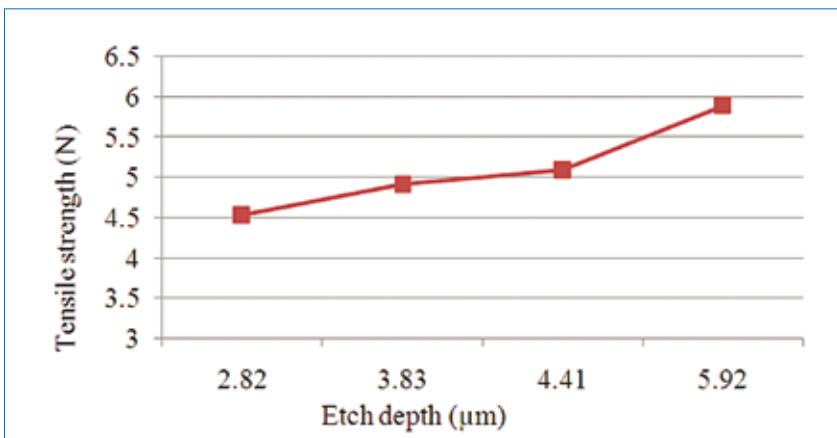


Figure 6. Bus-bar tensile strength for etch depths of 2.82μm, 3.83μm, 4.41μm and 5.92μm.

temperature, but there is little relation to surface conditions.

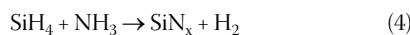
**Influence of etch depth on thickness of the PECVD film**

A tube-type plasma-enhanced chemical vapour deposition (PECVD) machine is used to deposit the SiN<sub>x</sub> layer, and the reaction gases are SiH<sub>4</sub> and NH<sub>3</sub>. The film thickness is measured by ellipsometry, and the values obtained for the thickness are shown in Fig. 5. The results indicate that the thickness of the film is greater as the etch depth increases.

“The results indicate that the thickness of the film is greater as the etch depth increases.”

The PECVD coating mechanism is described as follows [8]. High-frequency RF electric fields ionize the reaction gases to generate electrons. After several collisions, the reaction gases generate a large number of photons, electrons, ions and chemically reactive groups. Finally,

high-density plasma is formed in a closed chamber. Active groups are deposited on the wafer surface and react to form an SiN<sub>x</sub> film layer on it, which will reduce light reflection. The reaction equation is:



Because plasma deposition technology is used, wafer surface morphology has an important effect on SiN<sub>x</sub> film thickness. When the etch depth is greater, the surface

etch pits are larger and circular. This surface morphology has a smaller area and causes the film thickness to increase.

**Influence of etch depth on bus-bar tensile strength**

The most popular crystalline silicon solar cells produced today have two or three bus bars on both the front and rear sides, with electrodes for transferring the electricity. Screen printing is used, followed by co-firing, to form the bus-bar contact with the silicon. In the process of making modules, a welding rod needs to be attached to the bus bar to concatenate the cells one by one, and it is important to ensure adequate contact between the bus bar and the silicon. The tensile strength of the bus bar was measured in order to find out the relationship between etch depth and tensile strength. The bus-bar tensile strength was found to be greater as the etch depth increased, as shown in Fig. 6.

“... the bus-bar tensile strength was greater as the etch depth increased.”

SEM images were taken to analyze the contact of the silver paste of the bus bar with the wafer surface. Fig. 7 shows the sectional views of this contact for groups A and D. Group A, which had an average etch depth of 2.82μm, is seen to have much narrower etch pits, which may be caused by the inability of the silver paste to pass through the pits to form a better contact with the silicon, resulting in a lower tensile strength. On the other hand, Group D, with an average etch depth of 5.92μm, shown in the right image of Fig. 7, has a higher tensile strength. This is due to the larger etch pits and therefore better contact.

**Influence of etch depth on solar cell efficiency**

Energy transfer efficiency is the most important electrical property for solar cells, so it is important for industrial mass production to determine the

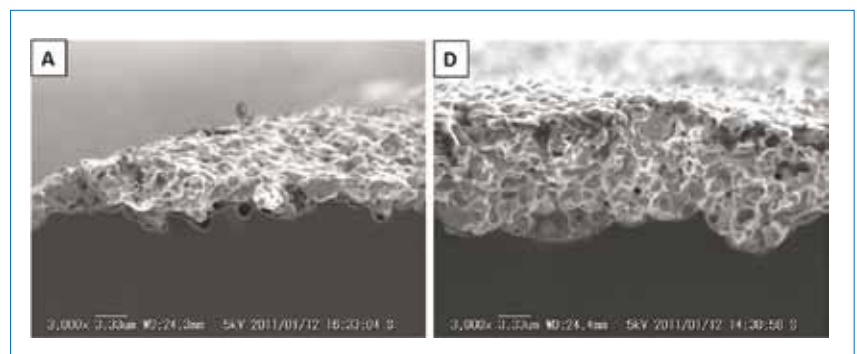


Figure 7. SEM images of bus-bar contact sections for different etch depths. Left: group A with etch depth 2.82μm. Right: group D with etch depth 5.92μm.

Test group	A	B	C	D
$V_{oc}$ [V]	0.617	0.617	0.620	0.619
$I_{sc}$ [A]	8.406	8.460	8.474	8.417
$R_s$ [ $m\Omega$ ]	3.192	3.039	3.072	3.062
$R_{sh}$ [ $\Omega$ ]	87.16	106.82	108.16	117.62
$I_{rev}$ [A]	0.322	0.386	0.338	0.349
FF [%]	77.95	77.98	78.14	78.08
Eff [%]	16.61	16.73	16.87	16.72

Table 2. Electrical properties of the cells for the different etch-depth groups.

connection between etch depth and cell efficiency. Table 2 shows the efficiency results for different etch depths, and it is clear that the etch depth does have an effect on efficiency. The open-circuit voltage ( $V_{oc}$ ) initially rises with increasing etch depth, but at some point between  $4.41\mu\text{m}$  and  $5.92\mu\text{m}$ ,  $V_{oc}$  starts to drop. At the beginning, the saw-damage layer is considered to be the main influence on  $V_{oc}$  and is a minority carrier recombination centre. As the etch depth increases (groups A–C), the saw-damage layer decreases and  $V_{oc}$  and the short-circuit current ( $I_{sc}$ ) increase remarkably. So, according to the  $V_{oc}$  values, it is known that the saw-damage layer is totally removed at an etch depth of  $\sim 4.41\mu\text{m}$ . For groups C and D, when the etch depth continues to increase,  $I_{sc}$  decreases. This is because the etch pits become larger and the surface reflection becomes greater. The best  $V_{oc}$  and  $I_{sc}$  are achieved when the etch depth is  $\sim 4.41\mu\text{m}$ . As mentioned above, this is due to the surface having a lower reflectance around this etch depth and the saw-damage layer being totally removed as well. Furthermore, the best efficiency is obtained when the etch depth is  $\sim 4.41\mu\text{m}$ .

## Conclusions

For mc-Si solar cells, in a certain etch-depth range, the surface reflectance decreases as the etch depth decreases, and vice versa. At the same time as the etch depth increases, the etch pits become larger and circular. Moreover, as the etch depth increases, the anti-reflecting film thickness shows an increasing

trend and the bus-bar tensile strength is improved. Experiments also show that the diffusion sheet resistances are not linearly dependent on surface morphology. The relationship between solar cell efficiency and etch depth was determined, resulting in a best etch depth of  $\sim 4.41\mu\text{m}$  for our mc-Si wafer samples. Around this etch depth, the saw-damage layer has been completely removed, while the surface still has a low reflectance. In parallel, it should be noted that the wafer surface morphology will change continually with the development of silicon crystalline growth and silicon ingot cutting technologies. Therefore the best etch depth should be regularly checked and revised accordingly.

## References

- [1] Stensrud, E. et al. 2005, "Acidic texturing of multicrystalline silicon wafers", *Proc. 31st IEEE PVSC*, Lake Buena Vista, Florida, USA, pp. 1309–1312.
- [2] Seidel, H. et al. 1990, "Anisotropic Etching of Crystalline Silicon in Alkaline Solutions", *J. Electrochem. Soc.*, Vol. 137, pp. 3626–3632.
- [3] Hauser, A. et al. 2005, "A simplified process for isotropic texturing of mc-Si", *Proc. 3rd World Conf. on PV Energy Conv.*, Osaka, Japan, pp. 1447–1450.
- [4] Cao, Y. et al. 2011, "Study of dark lines on the polycrystalline silicon solar cell and their influence on cell electrical properties", *Photovoltaics International*, 11th Edn, pp. 64–69.
- [5] Schneider, D. et al. 2002, "Quality control of ultra-thin and super-hard

coatings by laser-acoustics", *Surf. Coat. Tech.*, Vol. 153, pp. 252–260.

- [6] Liu, X. et al. 2004, "The principle and application of testing sheet resistance using four-point probe techniques", *Semiconductor Technology*, July, pp. 1094–1097.
- [7] Guan, X. 2003, *Fundamentals of Silicon Integrated Circuit Technology*, Peking University Press, Beijing, p. 65.
- [8] Wang, X. et al. 2002, "Research progress in SiN for multicrystalline silicon solar cells", *Materials Review*, March, pp. 23–25.

## About the Authors

**Rui Tong** obtained a master's degree in material physics and chemistry from the Nanjing University of Science and Technology. He has been with Motech for two years and is currently working in the R&D division. His main research area is c-Si solar cells.

**Jiayi Liu** studied at Zhejiang University and was awarded a master's degree in physics in 2007. He joined Motech in June 2010 as a senior engineer in the R&D division. In his current work he focuses mainly on wafer surface texturing.

**Stone Shih** has been the director of the R&D division of Motech (Suzhou) since June 2010. Prior to joining the company, he gained 11 years' experience as manager of the Material Analysis Department at UMC Co., worked for one year as manager of the Reliability Department at FOXCONN, and spent two years at the NCU Instrument Centre. He holds both a Ph.D. in material engineering from TUST and a master's degree in chemical engineering from NCU. His research interests include cell design and characterization, particularly of high-efficiency solar cells.

## Enquiries

Rui Tong  
Motech Renewable Energy Co. Ltd.  
No. 1, Mao-di Rd  
Kunshan City  
Jiangsu Province  
P. R. China 215316  
Email: tongruihuainan@163.com